

ALMA MATER STUDIORUM · UNIVERSITY OF BOLOGNA



School of Science
Department of Physics and Astronomy

Measurement of Muon Lifetime

Supervisors:

Prof. Luigi Guiducci
Dott. Marco Garbini
Dott. Federica Primavera
Dott. Marco Selvi

Submitted by:

Danish Alam
Robin Pelkner
Daniele Rossi

Academic Year 2021/2022

Abstract

In this experiment, we studied cosmic muon decays using plastic scintillator detectors. We aimed to obtain the muon lifetime by stopping the muon and measuring its decaying at rest to an electron. The experimental signature was given by a signal from the muon decay, followed by a delayed signal coming from the electron. We selected muon event candidates and subsequently identified events with a clear sign of their decaying. Muon lifetime is obtained from a fit to their decay time distribution. We also discussed the experimental setup and detection techniques, taking data and analysing these data to estimate the muon lifetime.

Contents

1	Introduction	1
1.1	General introduction to muons	2
1.2	Muons from cosmic ray showers	2
2	Experimental Setup	4
3	Preliminary Measurements	7
3.1	Working Voltage for the Photomultipliers	7
3.2	Threshold measurements	8
3.3	Delay Curve	10
3.4	TDC calibration	10
4	Trigger Logic and Data Taking	12
5	Data Analysis	13
6	Final Results and Conclusions	14
6.1	Analysis of each plane	14
6.2	All planes	16
6.3	With bound Muons	16
A	Threshold voltages of the PMTs	19
B	TDC calibrations	23

Chapter 1

Introduction

This experiment aims to determine the lifetime of muons. Muons are produced by cosmic ray showers in the higher atmosphere. Incoming Protons interact with the atmosphere and produce pions, which can decay into muons that are reaching the surface of the earth.

In this experimental setup, the incoming muons are slowed down and stopped by layers of iron and then detected with plastic scintillators.

This report is structured as follows: in this chapter, an introduction to the physical aspects of muons is given. Chapter 2 describes the used components and the experimental setup. In Chapter 3 the preliminary measurements for the calibration of the setup are described and their results are discussed. Chapter 4 discusses the composition of the experiment and the process of data taking, while Chapter 5 presents the data analysis. Chapter 6 concludes this report.

1.1 General introduction to muons

The standard model of elementary particles differentiates between quarks, leptons, and bosons. Quarks, as well as leptons, can be divided into three generations. The muons and the antimuon respectively are the second generation of leptons together with their associated neutrinos. Like the electron, muons have spin 1/2 and a negative elementary charge (a positive elementary charge for the antimuon). Although the similarities, they differ concerning their masses and their lifetimes.

While the electron is a stable particle, the muon has a finite lifetime, which this experiment is supposed to measure. The lifetime, given as an average result of past measurements, is $\tau = (2.196\,981\,1 \pm 0.000\,002\,2) \mu\text{s}$. Their mass is $m_\mu = (105.658\,374\,5 \pm 0.000\,002\,4) \text{ MeV}$, which is 206 times the mass of the electron [2].

1.2 Muons from cosmic ray showers

Muons are naturally produced in cosmic ray showers. The cosmic ray is mostly protons, but also electrons and atomic nuclei. These particles originate in various galactic and intergalactic sources like the sun, the Milky Way, and other galaxies. When a cosmic particle (e.g; Proton) strikes and interact the atmosphere, it produces a hadronic shower. The protons hadronize mostly into π mesons, because they are the lightest mesons, but also into K mesons and other hadrons. Due to their short lifetimes, Pions and Kaons also decay into muons via the weak interaction.

$$\begin{aligned}\pi^+ &\rightarrow \mu^+ + \nu_\mu \\ \pi^- &\rightarrow \mu^- + \bar{\nu}_\mu.\end{aligned}$$

This process is analogous to K mesons. The muons also only decay via the weak interaction as follows

$$\begin{aligned}\mu^- &\rightarrow e^- + \bar{\nu}_e + \nu_\mu \\ \mu^+ &\rightarrow e^+ + \nu_e + \bar{\nu}_\mu.\end{aligned}$$

Because the muons have a longer lifetime than pions. Hence, muons can reach the surface of the earth and can be detected through their decay. A schematic with typical processes, which lead to the production of muons, can be seen in Figure 1.1.

Once they arrive on the surface of earth, we can use experimental apparatus to detect them. The basic idea is that when a particle passes through matter they release part of its energy which is converted into new particles or radiation. The amount of released energy is described by the Bethe Bloch Formula:

$$-\frac{dE}{dx} = 2\pi N_a r_e^2 m_e c^2 \rho \frac{Z}{A} \frac{z^2}{\beta^2} \left[\ln\left(\frac{2m_e \gamma^2 v^2 W_{max}}{I^2} - 2\beta^2 - \delta 2 \frac{C}{Z}\right) \right]$$

The transferred energy from the particle to the atom will cause ionization or excitation of scintillating materials which convert these energies into visible lights. Then these visible light signals are converted into the electronic signals using the Photomultiplier tubes.

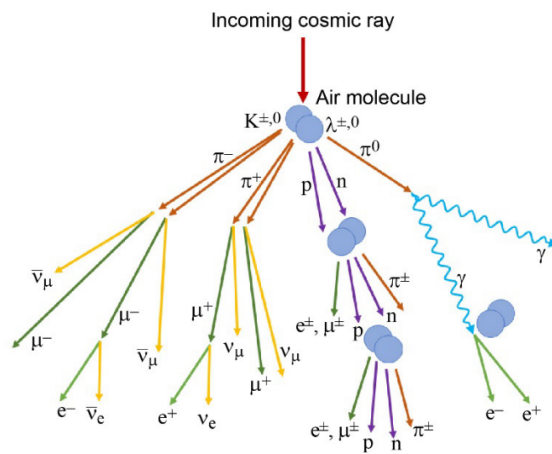


Figure 1.1: Typical shower processes after an incoming cosmic ray. The primary rays induce secondary particles by scattering with the molecules of the atmosphere. These secondaries can decay or scatter again with the atmosphere and produce more particles in the process. This is called a decay chain or a cosmic ray shower[1].

Chapter 2

Experimental Setup

In our experiment, we are detecting, mostly cosmic muons slowed by iron block(26 cm thick), using three layers of plastic scintillators (P0, P1 and P2) coupled to photo multipliers tubes (PMTs) each via a light guide. Due to the mechanisms of energy loss, from Bethe-Bloch formula, the minimum energy needed by muons to pass through 26 cm of iron is $E_\mu \approx 382\text{MeV}$ (considering muons at the minimum of ionization energy). Moreover, the block of iron reduces the electromagnetic component of the cosmic rays. The incoming muons are detected by the counters P0 and P1 which are thin enough to allow the muons to pass through. During the passage, these charged muons excite the vibrational motion of the molecules which, when de-energized, emit visible light photons(1 photon for every 100 eV deposited). The number of photons produced by scintillation is proportional (within statistical considerations) to the energy loss of the passing particle. Those photons will enter the PMT and produce electrons that form the electrical pulse we measure. The size of electronic pulse in a PMTs is proportional to the number of photons produced by scintillator. To maximize the numbers of photon that reach the photocathode of the PMTs, it is necessary that the scintillator, light guide and photomultiplier tube all be wrapped in reflective foil. Also, to block external light the assembly is then covered by black tape. After P1, the muons encounter a slab of iron in which some of them eventually stop and decay. If it happens, the emitted electron or positron is then detected by the surrounding counters. Therefore, what we would like to measure is the time interval between the signal for a stopped muon (' μ stop') and the detection of emitted electron or positron.

Other than the detector itself, we use a NIM (Nuclear Instrument Modules) and a CAMAC (Computer Automated Measurement And Control) crate with appropriate boards and modules. All algorithms and tunings of the experiment are done within the NIM crate and CAMAC is used for the read-out. The NIM modules which are used can be summarized as follows:

HV power supply:

N470 CEAN 4 Channel NIM Programmable High Voltage Power Supply.

This module is the power supply to the photomultiplier tubes.

Discriminator:

N840 CEAN 8 Channel Leading Edge Discriminator module; pulse width: 5-40 ns, and threshold 1-255 mV.

Given an analog input signal, the discriminator compares the amplitude with a threshold (in mV since it is amplitude). If the falling edge of the input signals overcomes the threshold then a LOGIC 1 signal is

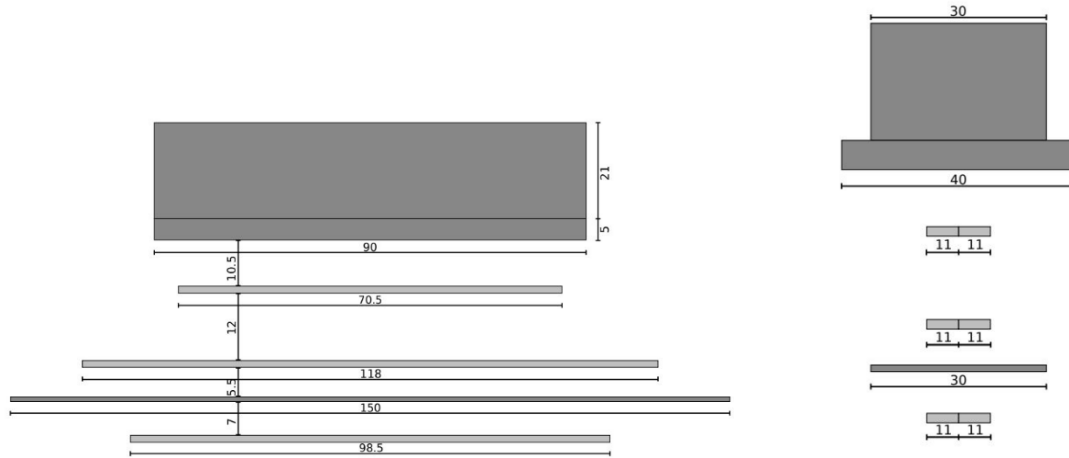


Figure 2.1: The experimental setup where it is shown in lateral and front view the absorber layers (dark grey) and the scintillator planes (light grey) with the dimensions in cm. Ref. Lab Manual Part 1

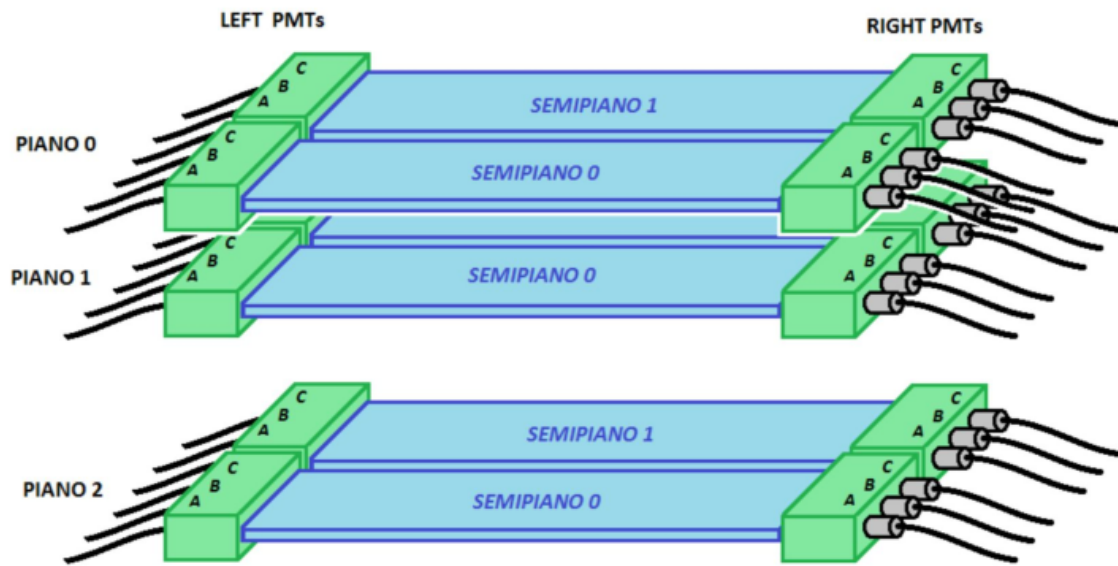


Figure 2.2: Scintillators with PMTs arranged in planes. Ref. Lab Manual Part 1

produced as output. If the signal is lower than the threshold, a LOGIC 0 is generated. The Standard LOGIC used by this module is the Nuclear Instrument Module Logic (NIM).

Logic Unit:

CAEN N405 3-fold logic unit module having 3 independent sections to perform logic AND/OR up to 4 logic signals in input.

It provides 1 linear OUT (width of the signals depending on input signals superposition), 2 fixed width (adjustable) OUT signals, 1 ANTI OUT signal, and 1 VETO input.

The first signal enters the LOGIC unit. During this time it is “1” the other signal arrives so there is Δt during which both signals are “1”. This means the signals coincide and an AND signal is produced.

FI/FO:

CAEN N625 Quad Linear FAN-IN FAN-OUT module

The module has 4 identical sections. Each section has 4 inputs that can be fed with analog signals. Then for each section, there are 4 identical OUT signals. If only one IN is used the 4 OUT are the replica of the IN signal. If more than one IN is connected then the OUTs provide the sum of the IN signals. So each of the 4 sections of this module can be used to replicate a signal 4 times (4 OUT).

Counter/Scaler:

CAEN N1145 Quad Scaler and Preset Counter/Timer

Count 4 NIM or TTL level signals for a given time interval defined by the user. The user can follow the countdown and read the number of counts on displays.

Dual Timer:// CEAN N93B Dual Timer module// This NIM module housing two identical triggered pulse generators which produce NIM and ECL pulses whose width ranges from 50 ns to 10 s when triggered. Output pulses are provided normal and complementary. Timers can be re-triggered with the pulse end marker signal.

Dual Delay:// CEAN N108A Dual delay module// Delay ranges from 0 to 63.5 ns (+ 1.6 ns offset) per section. The delay can be set in 0.5 ns steps. The delay lines are made up of calibrated coaxial cable stubs for high accuracy delay and do not require power supply.

Oscilloscope://

TDC:// CAEN mod. C414

A single width CAMAC unit housing 8 independent 12 bit time-to-digital conversion channels. The full scale time can be selected from 100 ns to 5 s via internal DIP switches. The time resolution ranges from 25 ps to 1.25 ns (respectively for 100 ns and 5 s full scale time range). The conversion time is 2.5 s per channel and it is reduced to 1.5 s for overflow channels. A CAMAC LAM is generated (if enabled) at the end of the conversion.

Chapter 3

Preliminary Measurements

3.1 Working Voltage for the Photomultipliers

As a first step, the optimal working voltages for the photomultipliers (PMTs) have to be found. Two PMTs were chosen for this measurement as a sample from the whole detector, R10B and R20A. It is important to choose PMTs from different planes to make sure the measured signal is due to a particle crossing the detector. A schematic for the measuring circuit is shown in Figure 3.1.

Only signals measured with both PMTs are taken into account. To determine these coincidences logic

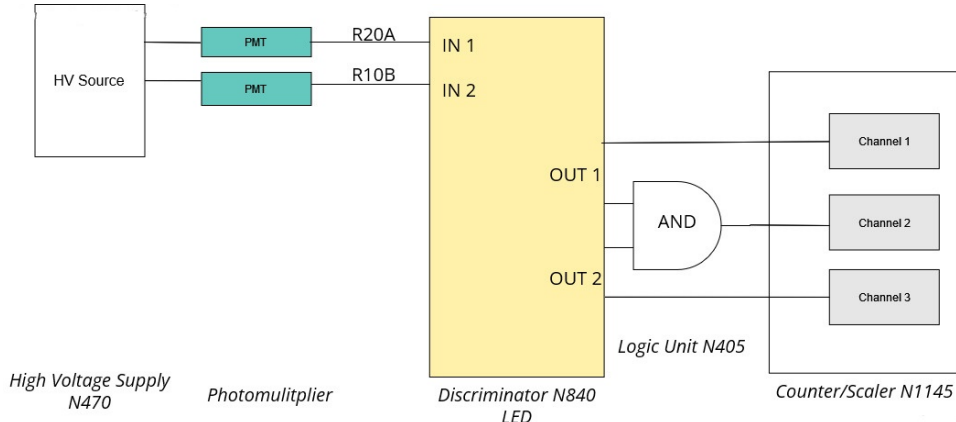


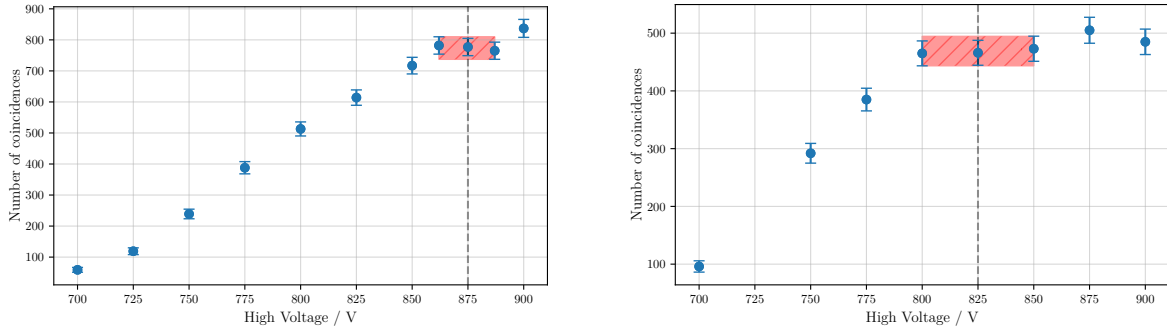
Figure 3.1: Schematic representation of the coincidence counting circuit for the PMTs. The signal propagation is from left to right starting with the PMTs and their high voltage supply and ending with the scaler.

signals are needed and for this, discriminators with a threshold of 40 mV are used. They convert the analogous signals of each PMTs into NIM standard signals. Using a logic unit module, we get the coincidences from the logic AND of both PMT signals. The NIM signals last for 40 ns each so the signals do not have to arrive at the same time but within 40 ns of each other because the muons arrive in the different planes at different times and not necessarily at the same distance from the PMTs. Furthermore,

the PMTs may have different delay times as well.

For the measurement, the R10B PMT works on a fixed high voltage of 775 V while the high voltage of R20A is varied from 700 V to 900 V. Each measurement lasts 200 s. The taken data is shown in Figure 3.2. A plateau can be found with 875 V corresponding to the middle value of it. This value is used as a fixed value for the R20A PMT when the voltage of the R10B PMT is varied in the same range of high voltages. The measurements for this PMT were each taken in 100 s due to time limitations. The central value of the plateau for this PMT is 825 V. Both measurements were also stopped when the PMTs are operating in the discharge region due to the high voltage to avoid damaging the PMTs.

The results are shown in Figure 3.2a and Figure 3.2b. All uncertainties are obtained assuming a Poissonian distribution, meaning $\sigma \propto \sqrt{N}$, where N is the number of coincidences. Because the output of the high voltage sources can fluctuate, the central values of the plateaus, 875 V for the R20A PMT and 825 V for the R10B PMT, can be used as the optimal working voltages to ensure a voltage output in the region of the plateau.



(a) Data of the R20A PMT. The central value of the plateau is 875 V.

(b) Data of the R10B PMT. The central value of the plateau is 825 V.

Figure 3.2: Measured number of coincidences regarding varying high voltages of the R10B PMT and the R20A PMT. The dashed line indicates the central values of each plateau. The striped red areas mark the found plateaus.

3.2 Threshold measurements

After the optimal working voltages was found, the determination of the optimal threshold voltage of the chosen PMTs started. A good determination of the threshold is necessary to suppress electronic noise on the one hand, but also to make sure that real signals are not filtered as well on the other hand. So the threshold can neither be too low nor too high.

Similar to the step before, a counting experiment of coincidences concerning the threshold voltages is conducted. This time the circuit arrangement is shown in Figure 3.3 is used. The PMTs are powered using the working voltages given in the laboratory as an average optimal working voltage for three PMTs.

In principle, the threshold of the discriminator of one plane is kept fixed at 15 mV, while the threshold of the other discriminator is being varied from 5 mV to 250 mV in irregular steps. Using a discriminator and

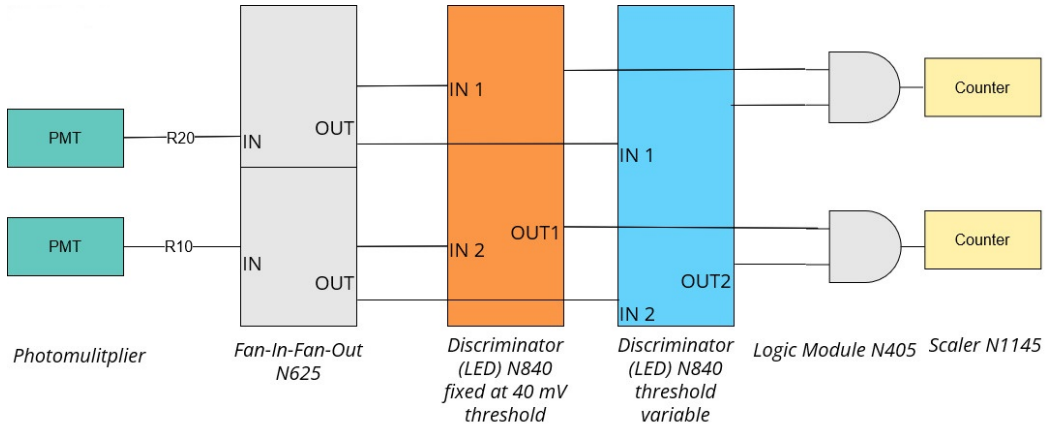


Figure 3.3: Schematic representation of the electronic circuit used to find the optimal threshold voltage. The signal flows from left to right, starting with the PMTs and Ending with the scaler.

a Fan-in-Fan-out system as shown in Figure 3.3, it is possible to vary the threshold of the discriminators of both PMT planes at the same time. Each counting measurement was conducted in 60 s.

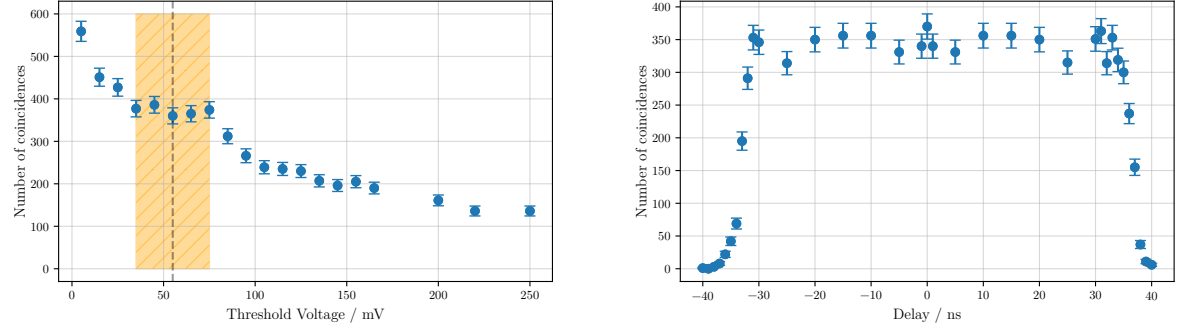
The results for the R10 and R20 planes can be seen in Figure 3.4. Results from other planes have to be taken from Appendix A, figures Figure A.1 to Figure A.6.

The data shows a higher number of coincidences at low threshold voltages, which decreases with

Table 3.1: Overview of optimal threshold voltages for each plane.

Plane	Voltage / mV	Plane	Voltage / mV	Plane	Voltage / mV
R00	50	R20	55	L01	55
R10	70	R21	55	L11	75
<i>R10</i>	45	L00	30	L20	50
R01	55	L10	35	L21	50
R11	60	<i>L10</i>	60		

rising voltages. This behavior is the same for all PMTs although not all curves show it that clearly. Also, a plateau of optimal threshold voltages can be seen. From the middle of this plateau, a threshold voltage has to be chosen as the optimal threshold value. As before the uncertainties will be taken into consideration using the Poissonian error. The optimal threshold voltages of all PMTs are shown in Table 3.1. Note that for the L10 signals and the R10 signals two measurements were taken. Thus, in these cases, only the value from the curve where it is easier to detect where the plateau is will be taken into consideration. The other values are marked italic in the tabular.



(a) Data of the R20 PMTs. The central value of the plateau is 55 mV.

(b) Data of the R10 PMTs. The central value of the plateau is 70 mV.

Figure 3.4: Measured number of coincidences concerning varying threshold voltages of the R10 PMTs and the R20 PMTs. The dashed line indicates the central values of each plateau. The striped orange areas mark the found plateaus.

3.3 Delay Curve

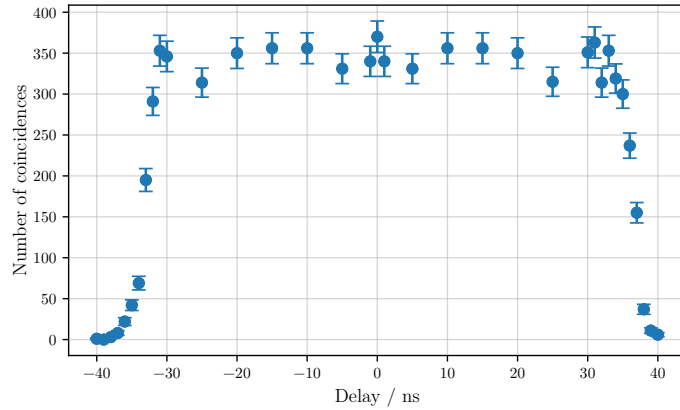


Figure 3.5: Delay Curve R10-R20.

3.4 TDC calibration

For all channels a linear function of the form

$$\text{TDC Time} = a \cdot t + b$$

is fitted to the data. This can be seen for all channels in the figures B.1 to B.8. The estimated parameters are shown in Table 3.2. In the following only channels 3, 4, 5 and 6 of each TDC will be used.

Table 3.2: Results of the TDC fits.

Channel	Slope a / TDCUnits/ns	Offset b /ns	$\chi^2/\text{d.o.f.}$
TDC 1			
1	0.754 ± 0.001	10 ± 5	0.037
2	0.766 ± 0.001	6 ± 5	0.038
3	0.747 ± 0.001	10 ± 5	0.037
4	0.758 ± 0.001	10 ± 5	0.037
5	0.738 ± 0.001	11 ± 4	0.036
6	0.719 ± 0.001	10 ± 4	0.035
7	0.732 ± 0.001	12 ± 4	0.034
8	0.742 ± 0.001	12 ± 4	0.035
TDC 2			
1	0.808 ± 0.001	44 ± 6	0.053
2	0.943 ± 0.005	48 ± 10	0.120
3	0.802 ± 0.002	37 ± 6	0.056
4	0.791 ± 0.002	43 ± 5	0.048
5	0.783 ± 0.001	15 ± 5	0.042
6	0.786 ± 0.001	29 ± 5	0.042
7	0.813 ± 0.002	44 ± 6	0.062
8	0.802 ± 0.002	39 ± 6	0.057

Chapter 4

Trigger Logic and Data Taking

Chapter 5

Data Analysis

Chapter 6

Final Results and Conclusions

6.1 Analysis of each plane

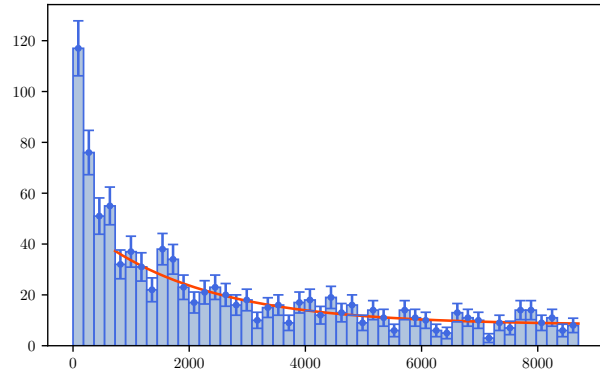
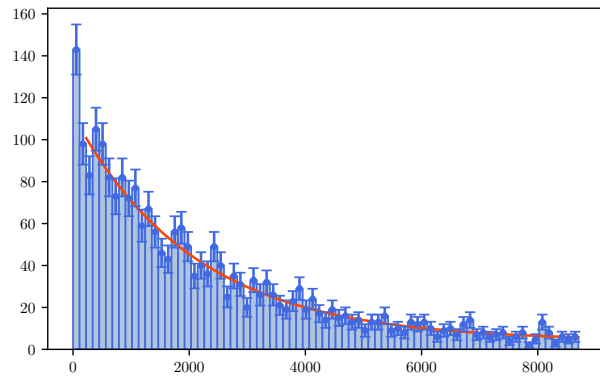
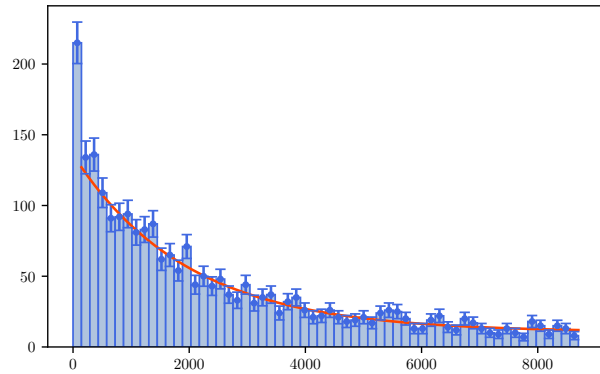


Figure 6.1: Plane 0.

Fit function:

$$N = a \cdot \exp\left(-\frac{t}{\tau}\right) + b$$

with N as the number of counts. Parameters in Table.

**Figure 6.2:** Plane 1.**Figure 6.3:** Plane 2.**Table 6.1:** Parameters of the Data analysis fits.

Plane	Entries	Parameter a	Parameter b	Lifetime $\tau/\mu\text{s}$	$\chi^2/\text{d.o.f.}$
P0	1030	41 ± 5	8 ± 2	2.0 ± 0.4	1.085
P1	2345	108 ± 3	4 ± 1	2.1 ± 0.1	0.893
P2	2510	125 ± 5	10 ± 2	2.0 ± 0.1	0.923
P1 + P2 + P3	5885	400 ± 11	30 ± 4	2.1 ± 0.1	0.959

6.2 All planes

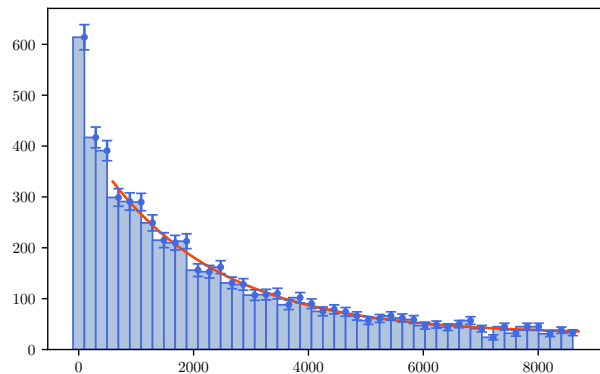


Figure 6.4: All Planes.

6.3 With bound Muons

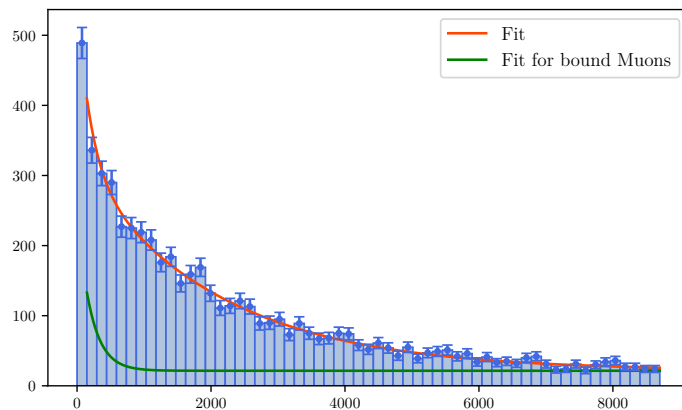


Figure 6.5: All Planes with bound Muons.

Parameters:

$$a = 228 \pm 13$$

$$b = 21 \pm 2$$

$$\tau_{\text{free}} = 2.1 \pm 0.1 \mu s$$

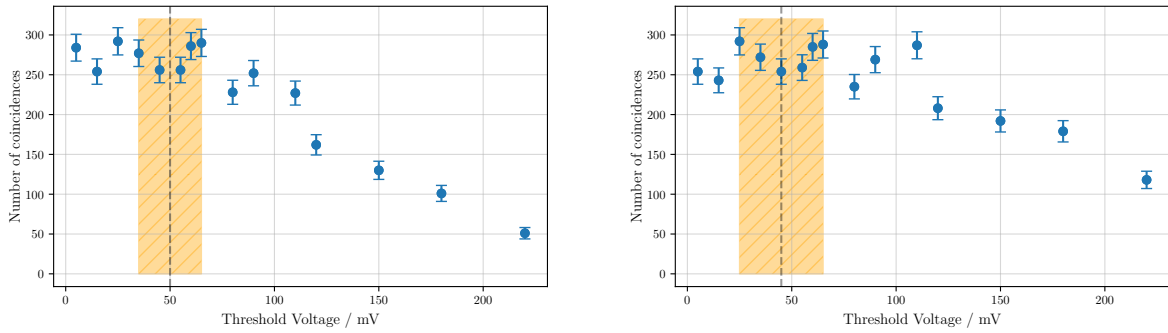
$$\tau_{\text{bound}} = 0.21 \pm 0.06 \mu s$$

Bibliography

- [1] J.D. Wrbanek and S.Y. Wrbanek. “Space Radiation and Impact on Instrumentation Technologies”. In: (2020).
- [2] P.A. Zyla et al. “Review of Particle Physics”. In: *PTEP* 2020.8 (2020). and 2021 update. doi: [10.1093/ptep/ptaa104](https://doi.org/10.1093/ptep/ptaa104).

Appendix A

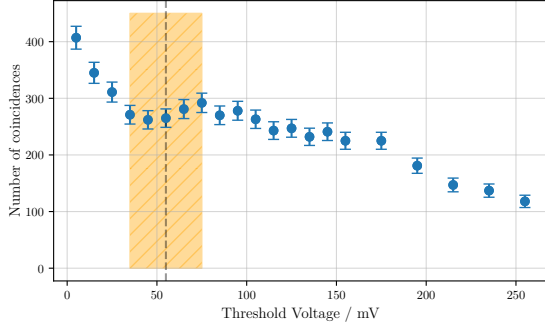
Threshold voltages of the PMTs



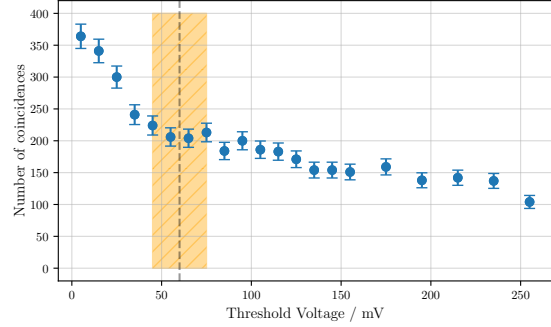
(a) Data of the R00 signal. The central value of the plateau is 50 mV.

(b) Data of the second measurement of the R10 signal. The central value of the plateau is 45 mV.

Figure A.1: Measured number of coincidences concerning varying threshold voltages of the R00 and R10 PMTs. The dashed line indicates the central values of each plateau. The striped orange areas mark the found plateaus.

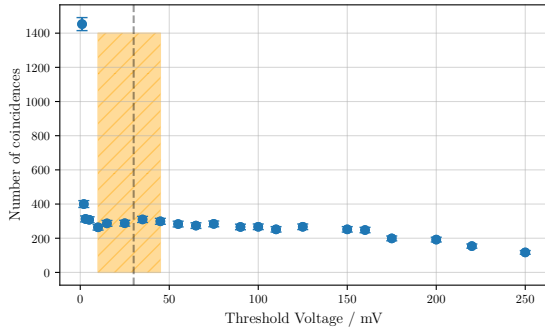


(a) Data of the R01 PMTs. The central value of the plateau is 55 mV.

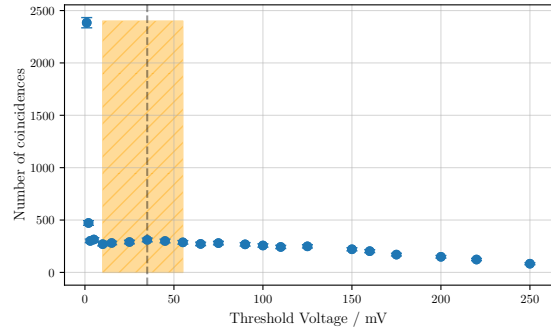


(b) Data of the R11 PMTs. The central value of the plateau is 60 mV.

Figure A.2: Measured number of coincidences concerning varying threshold voltages of the R01 and R11 PMTs. The dashed line indicates the central values of each plateau. The striped orange areas mark the found plateaus.

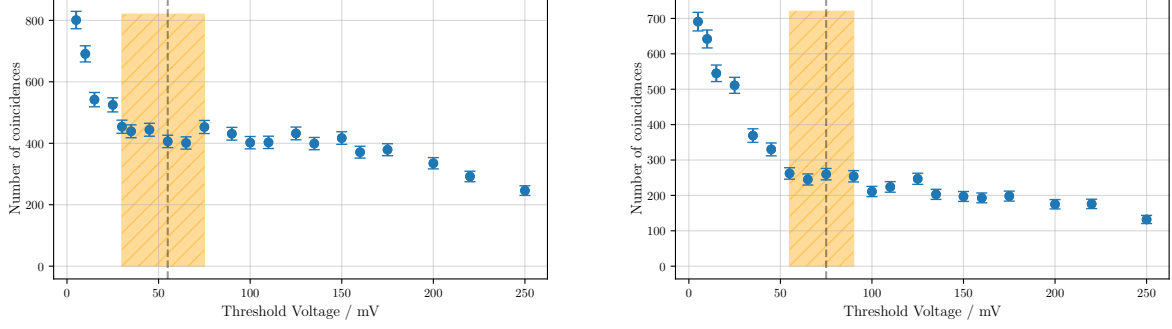


(a) Data of the L00 PMTs. The central value of the plateau is 30 mV.



(b) Data of the L10 PMTs. The central value of the plateau is 35 mV.

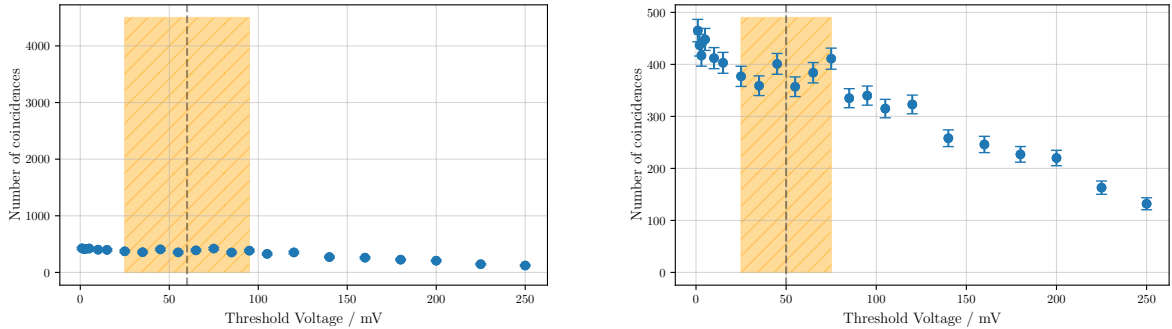
Figure A.3: Measured number of coincidences concerning varying threshold voltages of the L00 and L10 PMTs. The dashed line indicates the central values of each plateau. The striped orange areas mark the found plateaus.



(a) Data of the L01 PMTs. The central value of the plateau is 55 mV.

(b) Data of the L11 PMTs. The central value of the plateau is 75 mV.

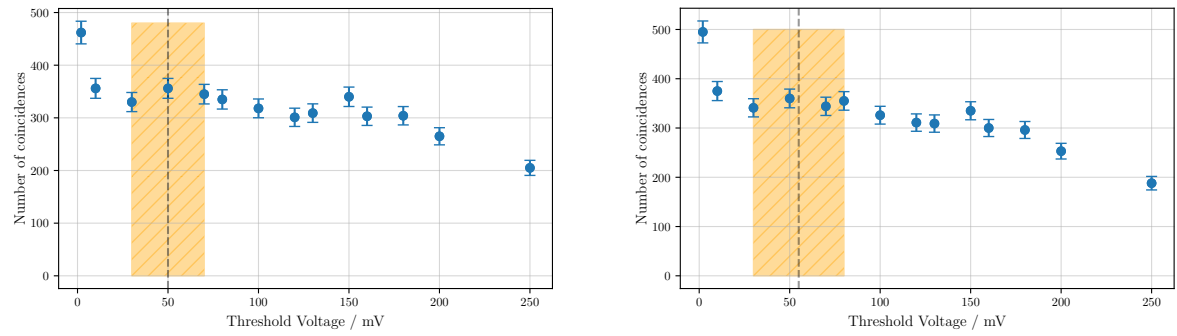
Figure A.4: Measured number of coincidences concerning varying threshold voltages of the L01 and L11 PMTs. The dashed line indicates the central values of each plateau. The striped orange areas mark the found plateaus.



(a) Data of the second measurement of the L10 PMTs. The central value of the plateau is 60 mV.

(b) Data of the L20 PMTs. The central value of the plateau is 50 mV.

Figure A.5: Measured number of coincidences concerning varying threshold voltages of the L10 and L20 PMTs. The dashed line indicates the central values of each plateau. The striped orange areas mark the found plateaus.



(a) Data of the L21 PMTs. The central value of the plateau is 50 mV.

(b) Data of the R21 PMTs. The central value of the plateau is 55 V.

Figure A.6: Measured number of coincidences concerning varying threshold voltages of the L21 and R21 PMTs. The dashed line indicates the central values of each plateau. The striped orange areas mark the found plateaus.

Appendix B

TDC calibrations

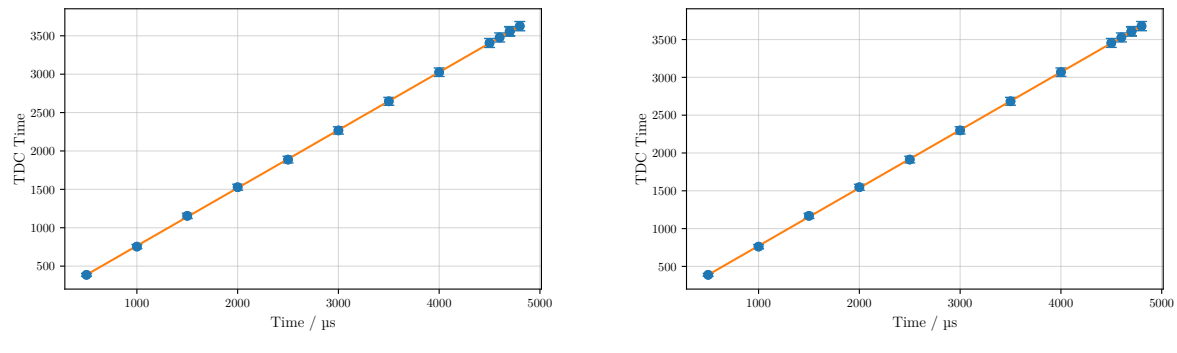
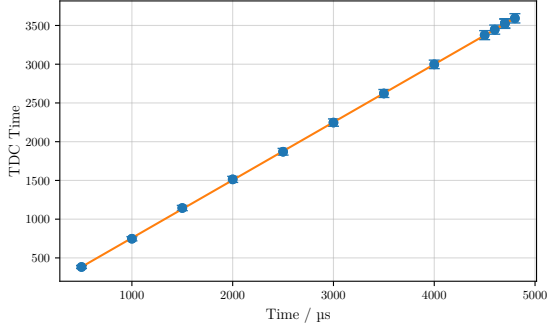
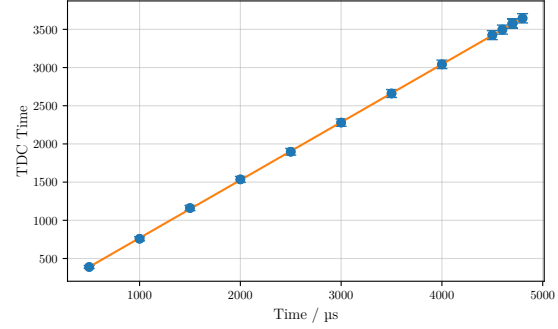


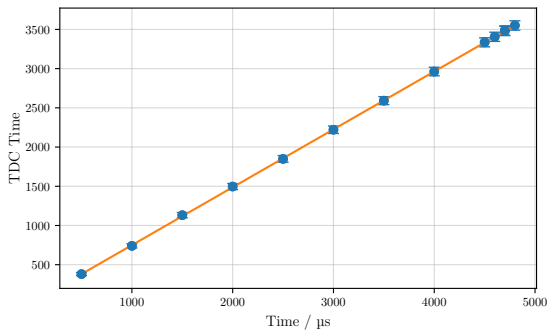
Figure B.1: Calibration Fits of Channel 1 and 2 of TDC 1.



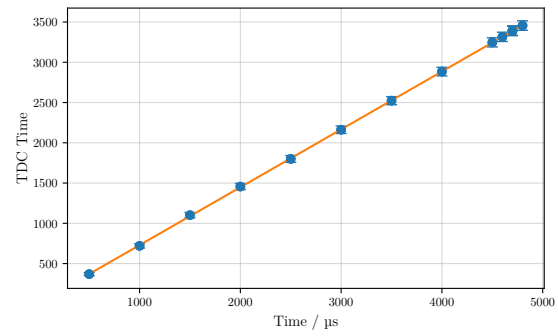
(a) TDC 1, Channel 3.



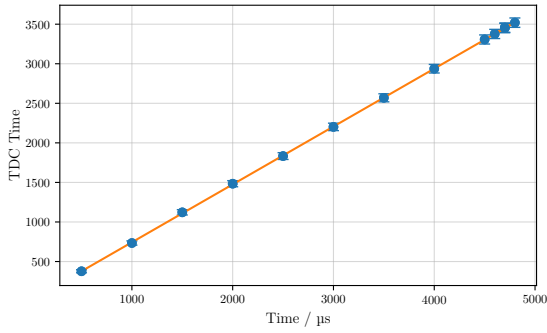
(b) TDC 1, Channel 4

Figure B.2: Calibration Fits of Channel 3 and 4 of TDC 1.

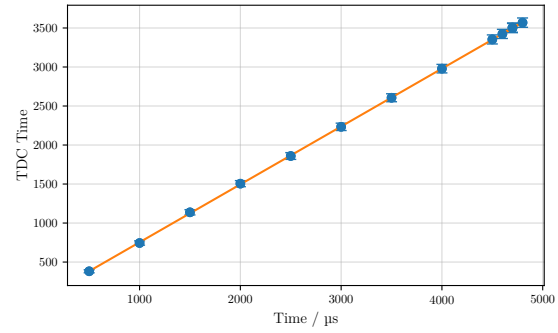
(a) TDC 1, Channel 5.



(b) TDC 1, Channel 6

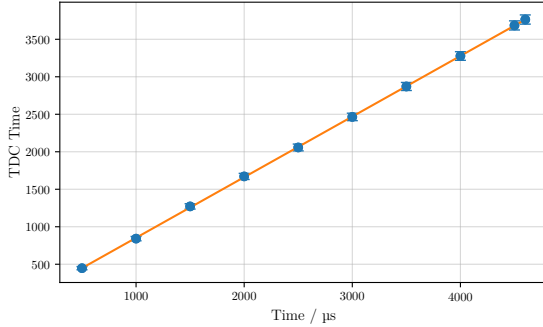
Figure B.3: Calibration Fits of Channel 5 and 6 of TDC 1.

(a) TDC 1, Channel 7.

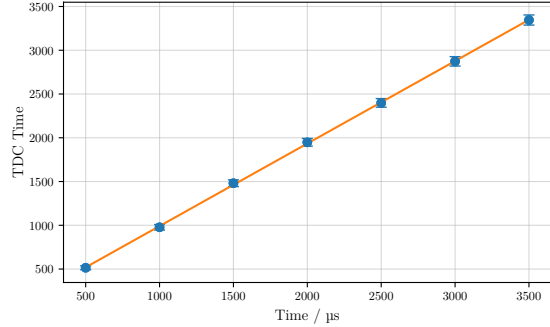


(b) TDC 1, Channel 8

Figure B.4: Calibration Fits of Channel 7 and 8 of TDC 1.

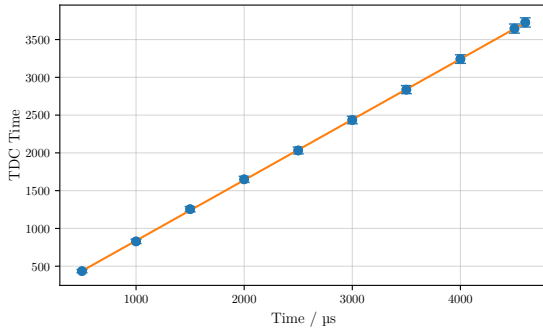


(a) TDC 2, Channel 1.

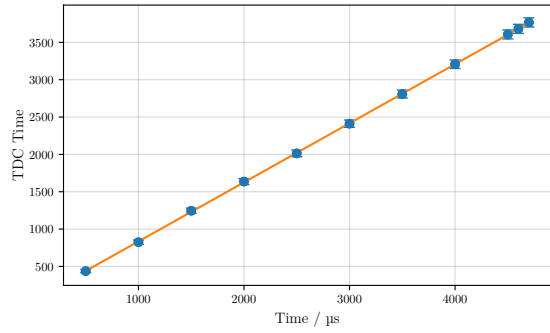


(b) TDC 2, Channel 2

Figure B.5: Calibration Fits of Channel 1 and 2 of TDC 2. Range of Channel 1 is limited to $4.6\text{ }\mu\text{s}$ and range of Channel 2 is limited to $3.5\text{ }\mu\text{s}$.

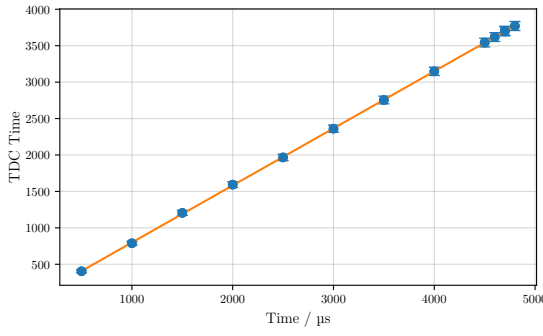


(a) TDC 2, Channel 3.

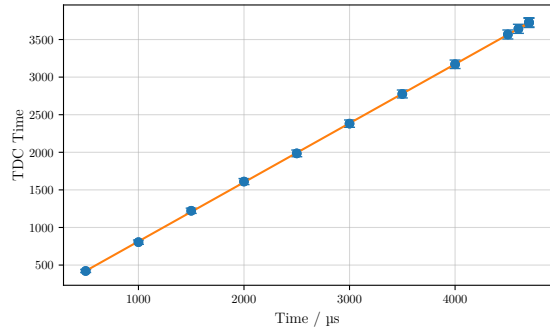


(b) TDC 2, Channel 4

Figure B.6: Calibration Fits of Channel 3 and 4 of TDC 2. Range of Channel 3 is limited to $4.6\text{ }\mu\text{s}$ and range of Channel 4 is limited to $4.7\text{ }\mu\text{s}$.



(a) TDC 2, Channel 5.



(b) TDC 2, Channel 6

Figure B.7: Calibration Fits of Channel 5 and 6 of TDC 2. Range of Channel 6 is limited to $4.8\text{ }\mu\text{s}$.

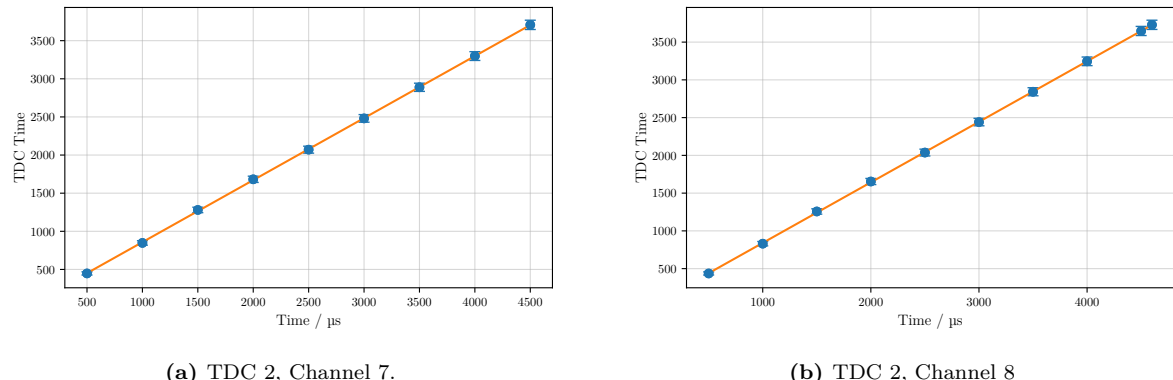


Figure B.8: Calibration Fits of Channel 7 and 8 of TDC 2. Range of Channel 7 is limited to $4.5\text{ }\mu\text{s}$ and range of Channel 8 is limited to $4.6\text{ }\mu\text{s}$.